On the criteria for the calculation of radial electric fields in stellarator plasmas

C. Gutiérrez-Tapia[1], J. J. Martinell[2], D. López- Bruna[3], A. V. Melnikov[4]

[1] Instituto Nacional de Investigaciones Nucleares, M éxico
[2] Instituto de Ciencias Nucleares (UNAM), México D.F., México
[3] Asociación EURATOM-CIEMAT, Madrid, Spain
[4] Research Center Kurchatov Institute, Nuclear Fusion Institute, Moscow, Russia

Abstract. Neoclassical (NC) transport theory has been considerably successful in describing effects observed in stellarators and heliotrons with quite different magnetic configurations Such effects include the formation of an electron heat transport barrier near the magnetic axis in low density discharges: the so called 'core electron root confinement' or CERC. In the steep gradient region near the edge, sheared ExB flows are expected to play an important role in the L-H transition. The development of analytical models, even if they are to be applied in complex geometries such as that of the Heliac, is still important because they are very fast and effective in calculating NC transport and electric fields, in comparison with more detailed, complex and time consuming numerical models, as shown by Kovrizhnykh for certain plasma density and of plasma temperature profiles. Thus, the ambipolar cubic equation admits only one stable solution if this solution is real for all values along the minor radius. The main objective of the present study is to show that the Kovrizhnykh criterion can be satisfied when the pressure profile consistency, obtained for several stellarators, is used. These complementary criteria become fundamental when calculating values of Er from the ambipolar equation. The temperature and density profiles are chosen in order to reproduce the experimental measurements of the plasma potential by means of the heavy ion beam probe (HIBP) diagnostic of the TJ-II stellarator during experiments with ECRH and NBI heating. The Er values have been analyzed and compared with experimental reported data. The Er roots and pressure profiles are discussed in the context of the L-H transition.

PACS numbers: 51.20.+d, 52.55.Hc, 52.25.Fi, 52.55.-s, 52.65.Pp

1. Introduction

The radial electric field E_r is generally considered as a key factor in determining the quality of transport in Stellarators and Tokamaks. In both types of devices there is compelling evidence that sheared ExB flows can suppress or considerably reduce turbulence, responsible in turn of large confinement losses. Even in the absence of developed turbulence, transport in stellarators is strongly dependent on E_r through the well known mechanisms of collisional transport, normally known as neoclassical (NC) transport theory. This theory has been successful in describing effects observed in stellarators and heliotrons with quite different magnetic configurations, like the formation of an electron heat transport barrier near the magnetic axis in low density discharges, i.e., the 'core electron root confinement' or CERC (e.g. LHD [1], CHS [2], W7-AS [3], TJ-II [4]). Moreover, in the steep gradients region near the edge, sheared ExB flows are expected to play an important role in the L-H transition. It is clear that NC transport is an important ingredient in the establishment of a radial variation of E_r and thus on the shear of ExB flows. So, in general, we can say that E_r is a very important element to understand both the anomalous and collisional transport mechanisms.

In the framework of the neoclassical transport theory, it is established, from the ambipolarity of toroidal systems, that the dynamic process of approaching the ambipolar state is simply a description of the momentum relaxation on a flux surface [5]. In the traditional neoclassical approach, the local radial electric field is determined by the roots of the ambipolarity condition of local (diffusive) particle fluxes

$$Z_i \Gamma_i^{nc} = \Gamma_e^{nc}, \tag{1}$$

if additional nonambipolar particle fluxes can be neglected. As the neoclassical transport coefficients, D_{jk}^{α}, depend on E_r, multiple roots (an odd number) may be obtained. These roots depend strongly on electron and ion temperatures profiles, as well as on density profiles. The problem of existence of multiple roots of equation (1) is related to the stability criteria of roots. One such criteria is proposed in [6] from a thermodynamic point of view, where it is found that for both radially local and nonlocal models, the stability of the equilibrium radial electric field is at the minimum of the generalized heat production rate. This idea was reported earlier in [7] where it is shown the existence of possible magnetohydrodynamic configurations that can be realized as 'most probable' states compatible with the existence of certain constraints imposed either experimentally or by some constants of motion.

For stellarators, with a complex magnetic field topology, full formulations do not exist either for the local (diffusive) neoclassical transport or for the nonlocal (convective) fluxes, e. g., driven by ECRH (electron cyclotron resonance heating) as well as for the NBI (neutral beam injection) heated discharges [8]. Nevertheless, the calculation of the radial electric field still being calculated traditionally by equation (1). In this work, we show the existence of two criteria followed from the stability of equilibrium to calculate the radial electric field at magnetic surfaces.

The first criterion arises from the ambipolarity of toroidal systems, that the dynamic process of approaching the ambipolar state is simply a description of the momentum relaxation on a flux surface [5]. After the proper force balance has been done there may still be flux surface flows in a local equilibrium. In stellarators usually the condition $|\mathbf{B}| = const$ is fulfilled [9]; then we can arrive at the condition $P = n_e T_e = const$ at magnetic surfaces. Also, as shown in [10], in equilibrium we obtain the relation $E_r = (Z_i e n_i)^{-1} \nabla P_i$. Thus, in order to calculate the radial electric field, the knowledge of the profiles of the ion density $n_i \approx n_e$ and pressure P_i is required, which could be obtained either experimentally or by modeling.

The second criterion is related with solutions of the ambipolarity equation (1). In neoclassical theory, within the lmfp (long mean free path) regime of small collision frequency, the diffusion and thermal conductivity coefficients depend on the electric field, yielding a cubic equation for the electric field. In some range of plasma density and electron and ion temperatures, equation (1) could have three different solutions, where one of them at least must be real (stable solution). In [11] it is argued that the field E_r undergoes discontinuous jumps, the particle and energy fluxes also turn out to be discontinuous and, accordingly, the particle and energy heat sources at these surfaces should have singularities of the δ-type, which, from the physical point of view, becomes hardly possible.

These two criteria become fundamental when calculating values of Er from the ambipolar equation. First, the main characteristics of the TJ-II stellarator, the HIBP diagnostic, the obtention of the experimental E_r and plasma potential, ϕ, in the three regimes identified: low, high and intermediate density, and the plasmas subject of this study are described in Sec. 2. In Sec. 3 we describe the basic physical criteria to solve the ambipolar equation. Next, in Sec. 4 the way in which E_r and ϕ are obtained is explained. A general discussion of the behavior of E_r and the NC model with respect to density in all the plasma regimes is given in Sec. 6. The work is summarized in the Conclusions (Sec. 7).

2. Experimental data

The TJ-II Heliac-type stellarator has a helical magnetic axis that winds around a circumference of radius $R_0 = 1.5$ m. The plasma has a bean-shaped cross section with average minor radius of $a \approx 0.2$ m and magnetic field at the axis $B_0 \approx 1.0$ T. The plasmas are always initiated with Electron Cyclotron Resonance Heating (ECRH); absorbed heating powers are normally $P_{\mathrm{ECRH}} = (200 - 400)$ kW and in the absence of other heat sources the line averaged densities are $\overline{n} = (0.3 - 1.0) \times 10^{19}$ m^{-3} with central electron temperatures $T_e(0) \sim (0.8 - 1.0)$ keV and ion temperatures of $T_i(0) \approx 90$ eV due to Coulomb heat exchange.

Additional heating and fueling can be obtained with the help of one or two neutral beam injectors (NBI) delivering port-through powers $P_{\mathrm{NBI}} = (300 - 500)$ kW each. Above line densities around 1.2×10^{19} m^{-3} the ECRH is no longer effective and the

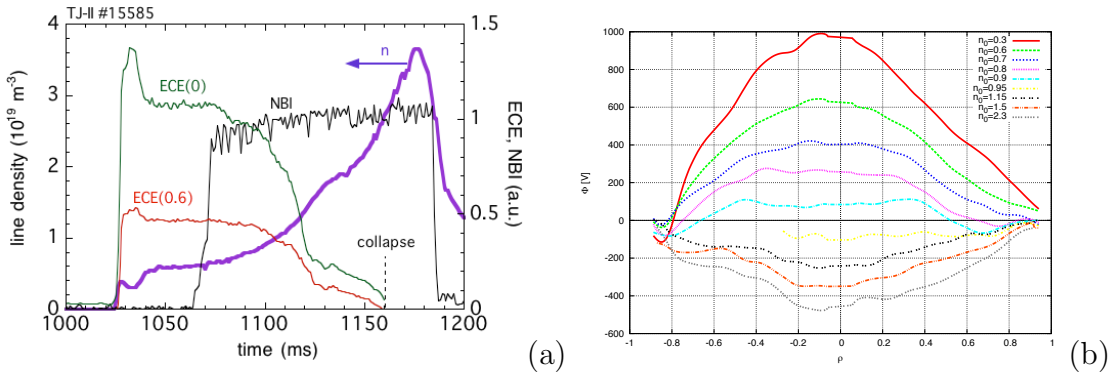

Figure 1. (a) Time signals of line density $\bar{n}$, ECRH heating and NBI heating during a NBI discharge (TJ-II #15585) with continuous density rise; (b) plasma potential profiles corresponding to the times indicated with vertical lines in (a) for several densities n_0 ($10^{19}m^{-3}$).

plasmas are sustained with NBI heating alone up to densities $\overline{n} = (2.0-5.0)\times 10^{19}$ m^{-3} with lower temperatures: $T_e(0) \sim 300$ eV and $T_i(0) \sim 120$ eV.

The electron density and temperature profiles are measured using Thomson Scattering diagnostic. The ion temperature is normally measured with the CX neutrals analyzer. T_i is quite homogeneous in the low density ECRH plasmas. In what follows, we use T_i based on the central values provided by the diagnostic, although we allow radial variations according to [12], i.e., the profiles are similar to n in low density — typically ECRH — discharges, but they are similar to T_e in high density discharges. The plasma potential in the bulk plasma is measured using the HIBP system described in [13].

According to Fig. 1 and following [14], three different types of plasma have been considered that represent different collisionality and they are characterized by the electron density:

LDHT (low density with high electron temperature): Low density ($\sim 0.6\times 10^{19}$ m^{-3}), high electron temperature ($T_e(0) \sim 1$ keV) and low ion temperature ($T_0 \sim 0.1$ keV) as normally found in ECRH plasmas. This regime is characterized by long mean free paths (LMFP) of the particles over most of the plasma, $\nu^* \ll 1$, giving rise to radial fluxes dominated by the contribution of bouncing particles due to the large magnetic ripple. ν^* is the collision frequency normalized to a model bounce frequency based on the rotational transform alone: $\nu* = \nu/\omega_b$, where we use a standard bouncing frequency based on the rotational transform and the transit frequency according to the thermal speed v_t, i.e. $\omega_b = \iota v_t/(2\pi R_0)$. In this regime the electrons, being much faster than the ions and having large magnetic moment due to the heating system (ECRH), dominate the radial fluxes causing E_r to be positive and $\phi \sim T_e/e$.

IDT (intermediate density and electron temperature): Intermediate densities ($\sim 10^{19}$ m^{-3}) and electron temperatures ($T_e(0) \sim 0.5$ keV), typically found in mixed ECRH +NBI plasmas, or in high density ECRH plasmas. It is a known fact in TJ-

II that in transiting from the low to the high density regimes described above the plasma goes through intermediate configurations of the potential as obtained by the HIBP measurements [15]. The corresponding plasmas have $n \sim 10^{19}$ m^{-3} and lower electron temperatures than in the typical ECRH plasma, although T_i remains on the order of 0.1 keV. The peculiarity of this regime in terms of plasma potential ϕ is that it changes sign somewhere in the plasma radius. These conditions can be obtained in relatively high density, albeit purely ECRH, plasmas; or in the transition from ECRH to NBI plasmas when both heating systems are active. It becomes clear that in the intermediate regime not only the plasma potential, but also the electric field, change sign inside the plasma. In particular, E_r starts becoming more negative near the plasma edge [16]. With increasing average Densities, the negative values of E_r cover also smaller radii until the entire plasma has a negative electric field.

HDLT (high density and low electron temperature): High density ($\gtrsim 2 \times 10^{19}$ m^{-3}) and low temperatures ($T_e(0) \sim 0.3$ keV, $T_i(0) \approx 0.12$ keV), corresponding to NBI plasmas. These plasmas have more comparable electron and ion temperatures and high density giving rise to shorter mean free paths for electrons and ions, satisfying $\nu^* \lesssim 1$, ions being closer to one. The contribution from helically trapped particles is now much smaller and the radial transport in these conditions is probably dominated by passing and toroidally trapped particles, which corresponds to the "plateau" regime. The larger tendency of ions to escape the plasma causes $E_r < 0$ in the entire plasma column.

3. Basic equations

First, it is worth saying that the observed radial fluxes in stellarators are normally larger than expected from standard NC transport considerations, particularly in regions far away from the plasma core. Thus, we do not attempt to make a NC comparison for the fluxes as they might be predominantly anomalous. However, as noted before, the non-ambipolar fluxes are in principle neoclassical, and thus we expect that the E_r obtained from NC transport explain the measured values reasonably well. The ability to reproduce the electric field should depend on the way the NC fluxes react to this field, which is different in the various models considered.

In the frame of the analytical model, the process followed is to give equilibrium radial profiles for $n(\rho), T_e(\rho)$ and $T_i(\rho)$, compute the fluxes Γ_e and Γ_i and obtain E_r. In order to cover the three regimes described in Sec. 2 we use a set of profiles that reproduce the main features of the experimental profiles shown in Fig. (2a , 3a, and 3b), as the density is varied. We have chosen profiles in the general form,

$$n(\rho) = n_a + n_0(1-\rho^a)^b; T_e(\rho) = T_{ae} + T_{0e}(1-\rho^{a_e})^{b_e}; T_i(\rho) = T_{ai} + T_{0i}(1-\rho^{a_i})^{b_i}, \quad (2)$$

where n_a, T_{ae}, and T_{ai} are the electron density, electron and ion temperatures at the boundary; n_0, T_{0e} and T_{0i} are the central electron density, electron and ion central temperatures, respectively. To find the constants involved in density and temperature profiles we have to satisfy two criteria: the existence of a stable plasma

equilibrium to be sure of the ambipolar state at magnetic surfaces and the existence of a unique real solution for the ambipolar equation (1). We start assuming that at steady-state the stable equilibrium is reached. Thus, provided that, in equilibrium, $\nabla P = \mathbf{j}\times\mathbf{B} = (\nabla\times\mathbf{B})\times\mathbf{B}$, if we consider that $|\mathbf{B}|$ is constant [9] along the radius, and considering that P is a flux function on magnetic surfaces then, we obtain that pressure $P = nT_e \approx const$ at magnetic surfaces, which allows to express the electron temperature T_e as an hyperbolic function of n. In our case, this hyperbolic equation is shown in Fig. 2a for the discharge TJ-II ♯15585 obtained in the form: $\tau_e = 1/(0.57+0.34\eta)$, with $\tau_\alpha = T_\alpha/T_{0e}$, $\eta = n/n_0$, $T_{0e} = 0.72$ and $n_0 = 0.61$.

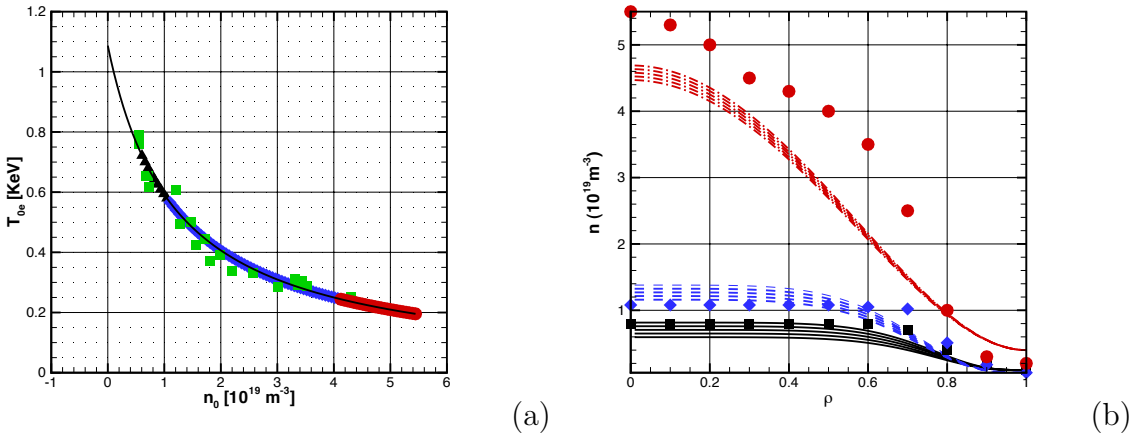

Figure 2. (a) Hyperbolic dependence between the central electron temperature and density (solid) and data from the set of Thomson Scattering profiles (squares). LDHT regime (inverted triangles), IDT regime (diamonds), and HDLT regime (circles); (b) density profile: LDHT regime (solid line) and experimental (squares), IDT regime (dashed line) and experimental (diamonds), and HDLT regime (dash-dotted lines) experimental (circles).

	n_a	n_0	a	b	T_{ae}	T_{0e}	a_e	b_e	T_{ai}	T_{0i}	a_i	b_i
(a)	0.1	≤ 1	6	4	0.1	≤ 0.72	1.5	2	.02	. 08	6	4
(b)	0.06	$(1,4]$	5	4	0.02	$(0.24, 0.57]$	1.5	2	. 04	.08	5	3
(c)	0.4	> 4	2	2	0.0001	< 0.24	4	1.5	.15	.12	5	1.5

Table 1. Constant values appearing in expressions (2) for different regimes of electron density and temperature ((a) LDTH regime, (b) IDT regime, and (c) HDLT regime) obtained from the fitting to an hyperbolic curve. Densities are expressed in $10^{19}\mathrm{m}^{-3}$, and electron and ion temperatures in KeV.

For this model, a simple magnetic geometry with a single helical harmonic

$$B_T = B_0[1-\epsilon_h(r)\cos(l\theta - M\varphi)]; \quad \epsilon_h(r) = \epsilon_0 I_l(Mr/R_0). \tag{3}$$

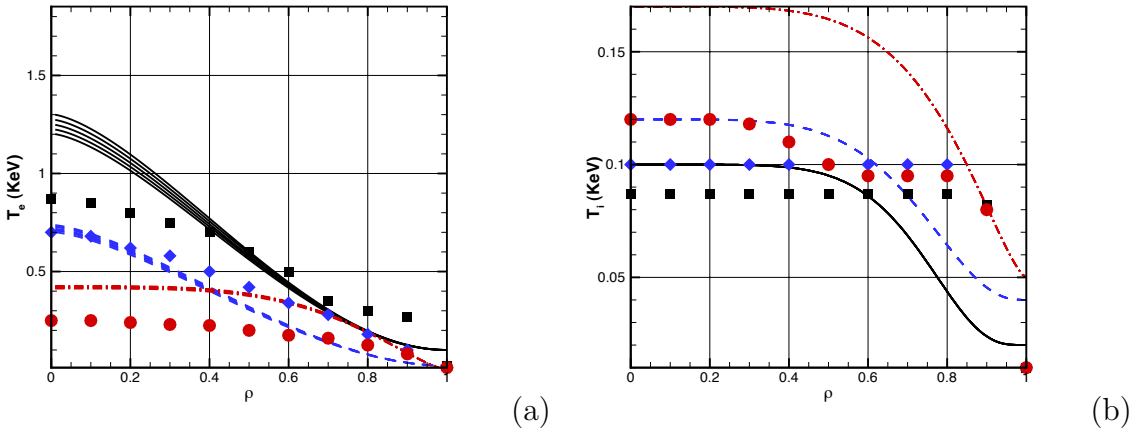

(a) (b)

Figure 3. (a) Electron temperature: LDHT regime (solid line) and experimental (squares), IDT regime (dashed line) and experimental (diamonds), and HDLT regime (dash-dotted lines) experimental (circles); (b) Ion temperature: LDHT regime (solid line) and experimental (squares), IDT regime (dashed line) and experimental (diamonds), and HDLT regime (dash-dotted lines) experimental (circles).

has been assumed; for the helical ripple we have taken $\epsilon_h = 0.134\rho$, which is adequate for TJ-II. It is implicitly assumed that all other fluxes (axi-symmetric and anomalous) are ambipolar. In these expressions, ϵ_0 is a constant defining the amplitude of the stellarator field, related to $\hat{\imath}(0)$, B_0 is the toroidal magnetic field at $\rho = r/a = 0$, and $I_l(x)$ is the modified Bessel function of the first kind

The particle fluxes Γ_j are given by equation

$$\Gamma_\alpha = -D_\alpha \left[\frac{n'}{n} + a_\alpha \frac{T'_\alpha}{T_\alpha} - \frac{q_\alpha E_r}{T_\alpha} \right] \tag{4}$$

when time dependent contributions associated to polarization currents are ignored, since we will be interested in steady state solutions. Following Kovrizhnykh [11], accounting for mean values for the radial electric field, the following limiting values of the a_α-coefficients are used,

$$a_i \cong 0.75, \quad a_e \cong 3.84,$$

corresponding to the situation where the mean potential $V_\alpha = Z_\alpha e R_0 E_r / T_{0e}$ is in the range $V_i^2 \ll V^2 \ll V_e^2$. When the toroidal net current $I_p \neq 0$, i.e. it arises a convective particle flux associated with the polarization current and thus the equilibrium becomes not stable, we must take into account the external particle sources Γ^{ext}. In this case, in addition to the ambipolarity equation (1), there is the particle balance equation

$$\Gamma_\alpha = \Gamma^{ext}, \tag{5}$$

where Γ^{ext} is the external charge source, and both have to be solved simultaneously. In our steady-state analytical approach, equation (1) is considered, which gives an algebraic equation of third degree in the dimensionless electric field V. This can be solved once

the equilibrium profiles $n(\rho)$ and $T_\alpha(\rho)$ are given. The resulting equation coming from (1) in steady state can be written as,

$$F(\rho, V) = V^3 + b(\rho)V^2 + c(\rho)V + d(\rho) = 0. \tag{6}$$

where the coefficients $b(\rho)$, $c(\rho)$, y $d(\rho)$ are given by

$$b(\rho) = \frac{1}{\mu\tau_i^{0.5} + \tau_e^{0.5}} \left[\mu t_i^{0.5}\tau_e L_e - \tau_e^{0.5} t_i L_i + 2\left(\mu t_i^{0.5} v_i - \tau_e^{0.5} v_e\right)\right], \tag{7}$$

$$\begin{aligned} c(\rho) = \frac{1}{\mu t_i^{0.5} + \tau_e^{0.5}} & \left[\mu u^2\eta^2\rho^{2-2l}\left(0.9\mu\tau_e^{-2.5} + t_i^{-2.5}\right)\right. \\ & \left. +2\left(\mu t_i^{0.5} v_i \tau_e L_e + \tau_e^{0.5} v_e t_i L_i\right) + \mu t_i^{0.5} v_i^2 + \tau_e^{0.5} v_e^2\right], \end{aligned} \tag{8}$$

$$\begin{aligned} d(\rho) = \frac{1}{\mu t_i^{0.5} + \tau_e^{0.5}} & \left[-\mu u^2\eta^2\rho^{2-2l}\left(0.9\mu\tau_e^{-2.5} t_i L_i - t_i^{-2.5}\tau_e L_e\right)\right. \\ & \left. +\mu t_i^{0.5} v_i^2 \tau_e L_e - \tau_e^{0.5} v_e^2 t_i L_i\right], \end{aligned} \tag{9}$$

where

$$L_\alpha = \frac{\partial \ln n}{\partial \rho} + a_\alpha \frac{\partial \ln T_\alpha}{\partial \rho}, \quad v_\alpha = l\varepsilon_h t_\alpha \rho^{l-1}, \quad \mu \approx 103, \quad \eta = n/n_{0e}, \quad t_\alpha = T_\alpha/T_{0\alpha}. \tag{10}$$

Depending on the values of the coefficients $b(\rho)$, $c(\rho)$, and $d(\rho)$, equation (6) can have three roots, $V_1(\rho), V_2(\rho), V_3(\rho)$, which have the form

$$V_1(\rho) = -\frac{1}{12}c_1 + \frac{c - \frac{1}{3}b^2}{c_1} - \frac{1}{3}b + \imath\frac{1}{2}\sqrt{3}\left[\frac{1}{6}c_1 + \frac{2c - \frac{2}{3}b^2}{c_1}\right], \tag{11}$$

$$V_2(\rho) = -\frac{1}{12}c_1 + \frac{c - \frac{1}{3}b^2}{c_1} - \frac{1}{3}b - \imath\frac{1}{2}\sqrt{3}\left[\frac{1}{6}c_1 + \frac{2c - \frac{2}{3}b^2}{c_1}\right], \tag{12}$$

$$V_3(\rho) = \frac{1}{6}c_1 - \frac{2\left(c - \frac{1}{3}b^2\right)}{c_1} - \frac{1}{3}b, \tag{13}$$

where $\imath$ is the imaginary unit and

$$c_1 = \left(36cb - 108d - 8b^3 + 12\sqrt{12c^3 - 3c^2b^2 - 54cbd + 81d^2 + 12db^3}\right)^{1/3}. \tag{14}$$

In general, two roots are stable and one is unstable but not all are real, as they should be to be acceptable. If the profiles are set arbitrarily, the solutions in certain regimes can present a jump in the E_r profile that corresponds to the transition from one root to another. As pointed out by Kovrizhnykh [11], this requires particle sources of the Dirac delta function type at the discontinuities which is unphysical. Therefore, these solutions should be discarded arguing that the corresponding $T_\alpha(\rho)$ and $n(\rho)$ profiles are not possible to obtain. The acceptable solutions should be those that result from the same root all across the radial coordinate. It is important to note that the edge region is the most sensible to yield multiple roots, particularly at low densities, in the sense that small variations in $T_e(\rho)$ there, can make a real root to appear or disappear.

The profiles that have been verified to yield one real root solutions all over the plasma are shown in Fig. 2a, in addition to the assumed ambipolarity at magnetic surfaces, allow us the determination of the interval of theoretical values of density and electron temperature located at each of regimes defined in § 2, shown in Figs. (2b, 3a, 3b) and resumed in Table 1.

4. Radial electric field and potential calculations

It is now clear that particle density and electron temperature are the main parameters in determining the electric radial field and plasma potential as it was shwn in [28]. The plasma potential profiles, $\phi(\rho)$, are obtained from E_r after radial integration from edge to magnetic axis imposing the constraint $\phi(a) = 0$. The results for the E_r-profiles in each case are shown in Figs. 4a. Although these are diverse, there are some general features that are common and in some sense reproduce the experimental profiles. In particular, the observed property of positive E_r at low density that changes to negative at large n, which is clear in Fig.4, is reproduced. The plasma potential behavior is shown in Figs. 4 b (compare with results of Fig. 1).

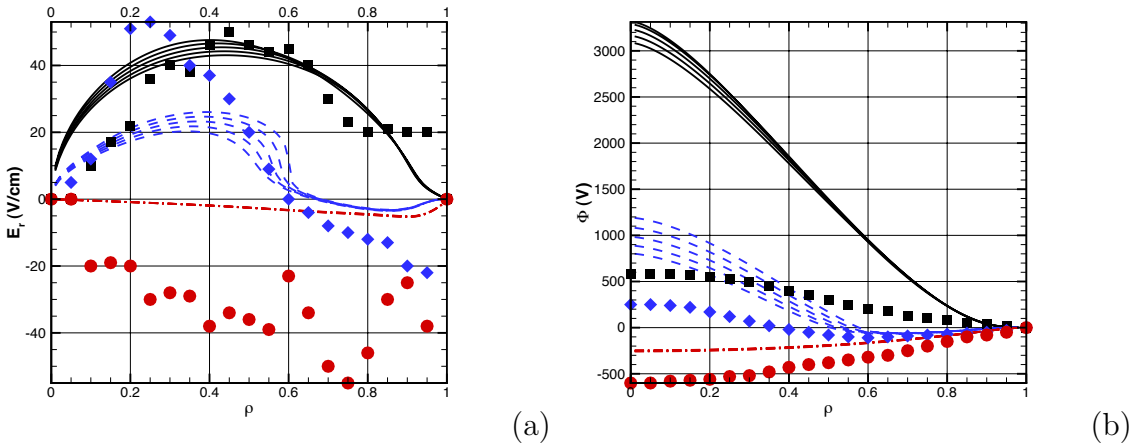

Figure 4. (a) E_r profiles: LDHT regime (solid line) and experimental (squares), IDT regime (dashed line) and experimental (diamonds), and HDLT regime (dash-dotted lines) experimental (circles); (b) ϕ profiles: LDHT regime (solid line) and experimental (squares), IDT regime (dashed line) and experimental (diamonds), and HDLT regime (dash-dotted lines) experimental (circles).

A common feature, already observed for TJ- II ECH plasmas [18], is that the plasma region where the electric field is inverted in passing from LDHT to HDLT plasmas —the regime of intermediate densities discussed above— is found in the interval $1 < n_0 < 4$ in agreement with the experiments. It should be stressed then that the basic NC assumptions, even for the complicated geometry of the TJ-II Heliac-type stellarator, provide a first overall explanation for the main experimental results shown.

The fact that the data in Fig. 4 includes the three regimes described above, implies that the heating method cannot be responsible for the behavior of $\phi(0)$ in this data set. It is worth mentioning, however, that T_e in these plasmas is linked to the density as shown in Fig. 2a. The relationship shown in Fig. 4b indicates that the plasma potential has dependencies related largely with the plasma parameters and the peculiarities of transport.

5. Pressure profile consistency

The self-consistency of pressure profiles [20, 21] of tokamaks is well known. Namely, [20] proposes the idea of canonical pressure and temperature profiles determined by the free energy functional, additional to the condition of total current and poloidal magnetic flux conservation [22, 23, 24]. It has been shown that, in stellarators, temperature profile consistency does not exist [25]. From the fundamentals of neoclassical transport theory, we know that from the ambipolarity of toroidal systems, the dynamic process of approaching the ambipolar state is simply a description of the momentum relaxation on a flux surface [5]. Thus, the ambipolar state at magnetic surfaces becomes in some way related to the pressure profile consistency.

In [26] several stellarators were compared resulting in the fact that, despite a large variety in electron temperature and density profiles obtained with a wide range of plasma parameters and heating, electron pressure profile consistency is observed. Also in this work it is suggested that at some point in radius take place the internal transport barrier (ITB) formation ($\rho \sim 0.4$). In [27] there were found conditions to obtain a stable equilibrium from the condition of current conservation and pressure consistency. These conditions allow the obtention of the constant which characterize the universal canonical profile $k \sim P_0^{-1} dP/d\rho \approx const$ for several magnetic field geometries.

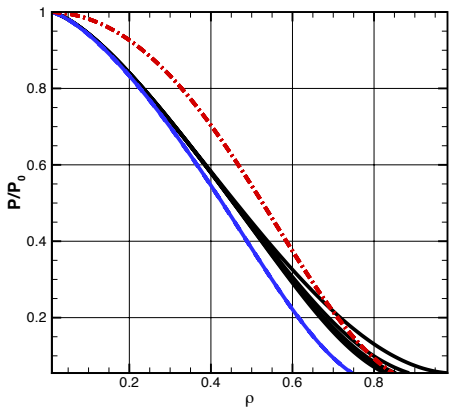

(a)

Figure 5. TJ-II normalized pressure profiles for data from Fig. (2a, 3a, 3b for several regimes. LDHT regime (solid line), IDT regime (dashed line) and HDLT regime (dash-dotted lines).

In our case, according to the two criteria used to obtain the radial electric field and the plasma potential, the normalized pressure profile is obtained from the relation $P \sim n \times T_e$. From Fig. 5 we note that as the pressure profile in the HDLT regime becomes wider that in the LDHT and IDT regimes, it is suggested that the L-H transition is achieved in these plasmas (see [29, 30]) partly due to the favorable neoclassical flows and electric field. However, a more detailed analysis in relation with the magnetic shear

is needed, as is reported in [27, 29].

6. Discusion

The plasma profiles are shown in Figs. (2b, 3a, 3b) for the three regimes: LDHT, IDT and HDLT. As it is shown in Fig. 2a these plasma parameters fall along a functional $n_0 - T_{0e}$-relation of the type found experimentally (Fig. 2a), which actually can be fitted by the model function, $\tau = 1/(0.57 + 0.34\eta)$. The corresponding real roots for $E_r(\rho)$ for each one of the cases just mentioned can be seen in Fig. 4a. The existence of real roots for all these cases corroborates the assertion about the importance of the functional dependence found on the basis of existence of the ambipolar state at magnetic surfaces. These results provide a relationship between density and electron temperature of the type $n_0 T_{e0} \approx const$ that has to be satisfied for actual plasma parameters, as one moves from one collisionality regime to another. This is conjectured because this condition points to a requirement to be fulfilled for the existence of continuous E_r profiles. If this is so, one has to understand why this condition arises. A possible explanation may be advanced if we first notice that this implies a constant plasma pressure near the center $p_0 = n(T_e + T_i)|_0 \approx n_0 T_{e0}$, or a constant averaged pressure, $\overline{p} \approx constant$. This may be justified by arguing that the MHD equilibrium condition ($p \sim p_B = B^2/8\pi$) requires the magnetic pressure to stay constant as the density is varied, which would be the condition associated with a constant magnetic well. Since it is a known fact that the magnetic well in most stellarators (and certainly in TJ-II) is quite wide and can be controlled fairly easily, containing most of the plasma core, this may be a plausible explanation. From this explanation it is to arrive to the existence of canonical pressure profiles observed in several stellarators [26] and founded in the framework of the generalized Grad-Shafranov equation [27]. Additionally, the E_r profiles and plasma potential, when compared to the corresponding experimental ones of Figs. 4a, and 4b, adjust fairly well in a qualitative fashion. From these figures, is important to note that the change from "electron" root to "ion" root is given in a continuous way, which becomes a demonstration that the bifurcation phenomena [31] does not exist in agreement with [11]

7. Conclusions

The results of calculations of the E_r field in the framework of neoclassical transport theory have been compared with experimental measurements of the plasma potential obtained with HIBP diagnostics in the TJ-II stellarator. Different collisionality regimes were analyzed which in general terms yield E_r profiles in agreement with the experiment. The analytical model based on the existence of the ambipolar state at magnetic surfaces and hence of the MHD stable equilibrium, and the existence of a real root of the ambipolar equation allow the determination of three characteristic intervals for density and electron temperature values in agreement with experimental observations. The E_r profiles and plasma potential, when compared to the corresponding experimental ones

of Figs. 4a, and 4 b, adjust fairly well in a qualitative fashion. From these results, it is important to note that the change from "electron" root to "ion" root is given in a continuous way, which becomes a demonstration that the bifurcation phenomena [31] does not exist in agreement with [11]. It is shown the pressure profile consistency in L-mode stellarator plasmas as well as a possible existence of the L-H transition in the HDLT regime observed in [29, 30].

Acknowledgements

This work was partially supported by RFBR Grants 10-02-01385 and 11-02-00667.

[1] K. Ida, T. Shimozuma, H. Funaba, et al. Phys. Rev. Lett. **91**, 085003 (2003).
[2] A. Fujisawa, H. Iguchi, T. Minami, et al. Phys. Rev. Lett. **82** (1999) 2669.
[3] U. Stroth, K. Itoh, S-I. Itoh, et al. J. Plasma Fusion Res. SERIES **4** (2001) 43.
[4] F. Castejón, V. Tribaldos, I. Garcia-Cortes, et al. Nucl. Fusion **42**, 271-280 (2002).
[5] K. C. Shaing, Phys. Fluids, **29**, 2231 (1986).
[6] K. C. Shaing, Phys. Fluids, **27**, 1567 (1984).
[7] D. Montgomery, L. Turner, and G. Vahala, J. Plasma Phys., **21**, 239 (1979).
[8] H. Maaßberg, et al. Phys. Plasmas, **7**, 295 (2000).
[9] V. Erckmann, et al., Nucl. Fusion, **43**, 1313 (2003).
[10] M. Coronado and J. N. Talmadge, Phys. Fluids B, **5**, 1200 (1993).
[11] L. M. Kovrizhnykh, Plasma Phys. Rep. **31**, 14 (2005).
[12] J. M. Fontdecaba , I. Pastor, et al., Plasma and Fusion Research **5**, S2085 (2010).
[13] A. V. Melnikov et al., Fusion Science and Technology. **51**, Jan. 2007.
[14] A. V. Melnikov, et al., VANT, ser. Termojadernyj Sintez, No.3, **55** (2011) (in Russian).
[15] I. S. Bondarenko et al., Czech. J. Phys., **50**, 1397 (2000).
[16] T. Happel, T. Estrada and C. Hidalgo, Europhys. Lett. 84, 65001 (2008).
[17] F. Tabarés et al., Plasma Phys. Control. Fusion **50**, 124051 (2008).
[18] D. López-Bruna, J. M. Reynolds, A. Cappa et al. *Programas Periféricos de ASTRA para el TJ-II.* Informes T écnicos Ciemat 1201, March 2010.
[19] D. López-Bruna, J. A. Romero, and F. Castej ón, *Geometría del TJ-II en ASTRA 6.0.* Informes T écnicos Ciemat 1086, August 2006.
[20] B. Coppi, Comments Plasma Phys. Contr. Fusion, **5**, 261 (1980).
[21] Yu. N. Dnestrovskij, et al., Nucl. Fusion, **46**, 953 (2006).
[22] B. B. Kadomtsev, Sov. J. Plasma Phys., **13**, 443 (1987).
[23] J. Y. Hsu and M. S. Chu, Phys. Fluids, **30**, 1221 (1987).
[24] D. Biskamp, Comments Plasma Phys. Contr. Fusion, **10**, 165 (1986).
[25] F. Wagner, et al., Phys. Plasmas, **12**, 072509 (2005).
[26] A. V. Melnikov, et al., *34th EPS Conf. on Controlled Fusion and Plasma Physics (Warsaw, 2007)*, P2.060 (2007).
[27] Y. N. Dnestrovskij, A. V. Melnikov, and V. P. Pustovitov, Plasma Phys. Control. Fusion, **51**, 015010 (2009).
[28] A. V. Melnikov, C. Hidalgo, L. G. Eliseev, e al., Nucl. Fusion, **51** 083043 (2011).
[29] T. Estrada, et al., Contrib. Plasma Phys., **50**, 501 (2010).
[30] J. Sánchez et al., Nucl. Fusion, **49**, 104018 (2009).
[31] A. Fujisawa, Plasma Phys. Contr. Fusion, **45**, R1 (2003).